A&A 635, A193 (2020)
https://doi.org/10.1051/0004-6361/202037526

Astronomy & Astrophysics

The population of hot subdwarf stars studied with *Gaia*

III. Catalogue of known hot subdwarf stars: Data Release 2*

S. Geier

Institut für Physik und Astronomie, Universität Potsdam, Haus 28, Karl-Liebknecht-Str. 24/25, 14476 Potsdam-Golm, Germany
e-mail: geier@astro.physik.uni-potsdam.de

Received 18 January 2020 / Accepted 13 February 2020

ABSTRACT

In light of substantial new discoveries of hot subdwarfs by ongoing spectroscopic surveys and the availability of new all-sky data from ground-based photometric surveys and the *Gaia* mission Data Release 2, we compiled an updated catalogue of the known hot subdwarf stars. The catalogue contains 5874 unique sources including 528 previously unknown hot subdwarfs and provides multi-band photometry, astrometry from *Gaia*, and classifications based on spectroscopy and colours. This new catalogue provides atmospheric parameters of 2187 stars and radial velocities of 2790 stars from the literature. Using colour, absolute magnitude, and reduced proper motion criteria, we identified 268 previously misclassified objects, most of which are less luminous white dwarfs or more luminous blue horizontal branch and main-sequence stars.

Key words. subdwarfs – stars: horizontal-branch – catalogs

1. Introduction

Hot subdwarf stars (sdO/Bs) are situated at the extreme blue end of the horizontal branch (HB), the extreme horizontal branch (EHB; Heber 1986). To evolve to the EHB, red giants must lose almost their entire hydrogen envelopes. This is best explained by various scenarios of binary mass transfer (Han et al. 2002, 2003; see Heber 2016, for a review). Although not initially recognised as such, sdO/B stars were discovered via photometric surveys of faint blue stars (Humason & Zwicky 1947; Iriarte & Chavira 1957; Chavira 1958, 1959; Haro & Luyten 1962; Green et al. 1986; Downes 1986). Subsequently, Kilkenny et al. (1988) published the first catalogue of 1225 spectroscopically identified hot subdwarf stars. Objective prism surveys obtaining low-resolution spectra detected many more hot subdwarfs (Hagen et al. 1995; Wisotzki et al. 1996; Stobie et al. 1997; Mickaelian et al. 2007; Mickaelian 2008). Østensen (2006) compiled a database containing more than 2300 stars.

Subsequently, the Sloan Digital Sky Survey (SDSS) provided spectra of almost 2000 sdO/Bs (Geier et al. 2015a; Kepler et al. 2015, 2016) and new samples of bright hot subdwarf stars were selected (e.g. Vennes et al. 2011). Furthermore, data from new large-area photometric and astrometric surveys have been conducted in multiple bands from the UV to the far-infrared.

This motivated us to compile a new catalogue of hot subdwarf stars (Geier et al. 2017a). We started with the catalogue of Østensen (2006) and added hot subdwarf candidates from several recent spectroscopic surveys (Mickaelian 2008; Østensen et al. 2010a; Geier et al. 2015a; Kepler et al. 2016; Gentile Fusillo et al. 2015; O'Donoghue et al. 2013; Kilkenny et al. 2015, 2016; Vennes et al. 2011; Oreiro et al. 2011; Perez-Fernandez et al. 2016; Luo et al. 2016) and unpublished sources. We cross-matched all those objects with large-area photometric and light curve survey catalogues. Proper motions were obtained from diverse ground-based surveys (see Geier et al. 2017a for details).

The spectroscopic catalogue of Geier et al. (2017a) has been used as an input catalogue for photometric (TESS; Stassun et al. 2018) and spectroscopic surveys (LAMOST; Lei et al. 2020); it has also been used to select stars for more detailed studies (Boudreaux et al. 2017; Carrillo et al. 2020). Furthermore, this previous catalogue has been used to determine selection criteria for an all-sky catalogue of hot subluminous star candidates selected from *Gaia* Data Release 2 (DR2; Gaia Collaboration 2018) by means of colour, absolute magnitude, and reduced proper motion cuts (Geier et al. 2019). In this work, I present Data Release 2 of the catalogue of known hot subdwarf stars.

2. Constructing the catalogue Data Release 2

2.1. Input data

In addition to the spectroscopically classified hot subdwarf stars from Data Release 1 (DR1) of this catalogue (Geier et al. 2017a), several new samples of hot subdwarfs have recently been published, most of which have atmospheric parameters and radial velocity determinations. Kepler et al. (2019) identified sdO/Bs in SDSS DR14 and Geier et al. (2017b) provided atmospheric parameters for a large sample of hot subdwarfs from SDSS DR7. However, the most important new source of yet undiscovered sdO/Bs is the LAMOST survey (Lei et al. 2018, 2019, 2020; Luo et al. 2019). It has to be pointed out that a lot of the recently published stars had already been classified and that there are large overlaps between the samples. By carefully cross-matching the new samples with the catalogue and each other, I found that 528 new sdO/Bs have been discovered since the publication of DR1.

New hot subdwarfs have also been identified in globular clusters (Latour et al. 2018), but owing to the different types of photometric and astrometric data available for those objects, they are not included in this catalogue. This means that the catalogue

* The catalogues are only available at the CDS via anonymous ftp to cdsarc.u-strasbg.fr (130.79.128.5) or via http://cdsarc.u-strasbg.fr/viz-bin/cat/J/A+A/635/A193

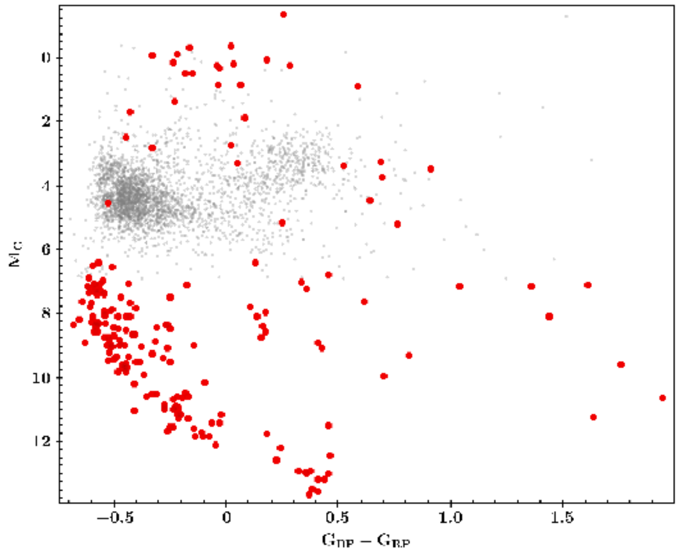

Fig. 1. *Gaia* colour–absolute magnitude diagram of the subsample with accurate parallaxes. Grey dots denote sdO/Bs and red dots show misclassified objects.

should be regarded as compilation of known hot subdwarf stars in the field.

2.2. Multi-band photometry

Near-ultraviolet (NUV) and far-ultraviolet (FUV) photometry were taken from the Galaxy Evolution Explorer (GALEX) All-sky Imaging Survey (AIS DR5; Bianchi et al. 2011). Optical photometry was obtained from *Gaia* DR2 in the G_{BP}, G_{RP}, and G bands (Gaia Collaboration 2018), the American Association of Variable Star Observers (AAVSO) Photometric All Sky Survey (APASS DR9; Henden et al. 2016) in the *VBgri* bands, the SDSS DR12 (Alam et al. 2015) in the *ugriz* bands, the Panoramic Survey Telescope and Rapid Response System (Pan-STARRS) PS1 survey (Chambers et al. 2016) in the *grizy* bands, the SkyMapper Southern Sky Survey DR1.1 (Wolf et al. 2018) in the *uvgriz* bands, and the Very Large Telescope Survey Telescope (VST) ATLAS (DR3; Shanks et al. 2015) and the Kilo-Degree (KiDS DR3; de Jong et al. 2015) ESO public surveys in the *ugriz* bands.

Near-infrared photometry was obtained from the Two Micron All-sky Survey (2MASS) All-Sky catalogue of Point Sources (Skrutskie et al. 2006) in the *JHK* bands, the United Kingdom Infra-Red Telescope (UKIRT) Infrared Deep Sky Survey (UKIDSS Large Area Survey DR9; Lawrence et al. 2007) in the *YJHK* bands, the Visible and Infrared Survey Telescope for Astronomy (VISTA) Hemisphere (VHS DR2; McMahon et al. 2013), and the VISTA Kilo-degree Infrared Galaxy (VIKING DR4; Edge et al. 2013) ESO public surveys in the $ZYJHK_s$ bands. Far-infrared photometry was obtained from the Wide-field Infrared Survey Explorer mission (WISE) AllWISE data release (Cutri et al. 2014) in the four WISE bands. Galactic reddening $E(B-V)$ and Galactic dust extinction A_V from the maps of Schlafly & Finkbeiner (2011) were also provided.

2.3. Gaia astrometry

Gaia DR2 (Gaia Collaboration 2018) provides precise coordinates, parallaxes, and proper motions (Lindegren et al. 2018), which have been included in the catalogue. Ground-based proper motions are no longer included.

2.4. Cleaning the catalogue

The data collected were used to identify and remove objects misclassified as hot subdwarf stars (Geier et al. 2017a). To separate all kinds of cooler objects, colour indices were used. Objects with SDSS colours $u-g > 0.6$ and $g-r > 0.1$, $\mathrm{NUV_{GALEX}} - g_{PS1} > 1.7$, SkyMapper $u-g > 0.9$ and $\mathrm{NUV_{GALEX}} - g_{APASS} > 2.0$ have been excluded if different indices were consistent. If only one of those indices was available, *Gaia* $G_{BP} - G_{RP} > 0.4$ was used as additional constraint.

Gaia DR2 provides us with accurate parallax distances with uncertainties smaller than 20% for distances up to about 1−2 kpc (Lindegren et al. 2018). Calculating the absolute magnitudes of all stars with accurate parallaxes, it was possible to identify misclassified white dwarfs (WDs) and also brighter objects such as blue horizontal branch (BHB) or main-sequence B (MS-B) stars (see Fig. 1).

To distinguish WDs from the more luminous and distant sdO/Bs, I also used the reduced proper motion method as outlined in Gentile Fusillo et al. (2015). The reduced proper motion $H = G + 5\log\mu + 5$ was calculated using the *Gaia* G magnitudes and proper motions because accurate *Gaia* proper motions are available for all stars in the catalogue. Stars with $H > 15$ are WD candidates and therefore excluded (Geier et al. 2017a). Most of the WD candidates identified in this work are also listed in the *Gaia* WD catalogue (Gentile Fusillo et al. 2019). Some bright BHB and MS-B stars have been identified from new follow-up spectra (Schneider et al., in prep.). The catalogue was also cross-matched with SIMBAD and misclassified objects known from the literature were also excluded.

The 268 misclassified objects are provided with their correct classifications as a separate catalogue. Based on their previous classifications as sdBs or sdOs and their colours, a tentative classification of the WD candidates as either DAB (hydrogen and possibly neutral helium lines) or DAO (hydrogen and/or ionised helium lines) candidates is provided. If there was no detailed classification before, they are classified as WD.

The final DR2 catalogue contains 5874 unique objects (see Fig. 2). Thanks to *Gaia*, which allows us to separate the WDs and bright MS-B stars very efficiently, BHB stars should now be the most important class of contaminant objects remaining in the catalogue.

2.5. Classification of hot subdwarfs

For spectroscopic and photometric classifications, we follow the scheme outlined in Geier et al. (2017a). The empirical scheme for the photometric classification by inspecting the locations of the subclasses in two-colour diagrams could be extended using new colour criteria based on multi-band photometry from PanSTARRS (Chambers et al. 2016) and SkyMapper (Wolf et al. 2018).

The SDSS- and SkyMapper-based colour classes should be regarded as the most trustworthy because the $u-g$ colour allows us to distinguish between sdB and the hotter sdO types better than a combination of NUV and g band (see Fig. 3). The updated colour criteria are provided in Table 1.

2.6. Spectroscopic parameters and radial velocities

The catalogue contains spectroscopic parameters such as effective temperatures, surface gravities, and helium abundances for 2187 stars from the literature; this is more than twice as many as in DR1. This fraction is still not complete because only papers

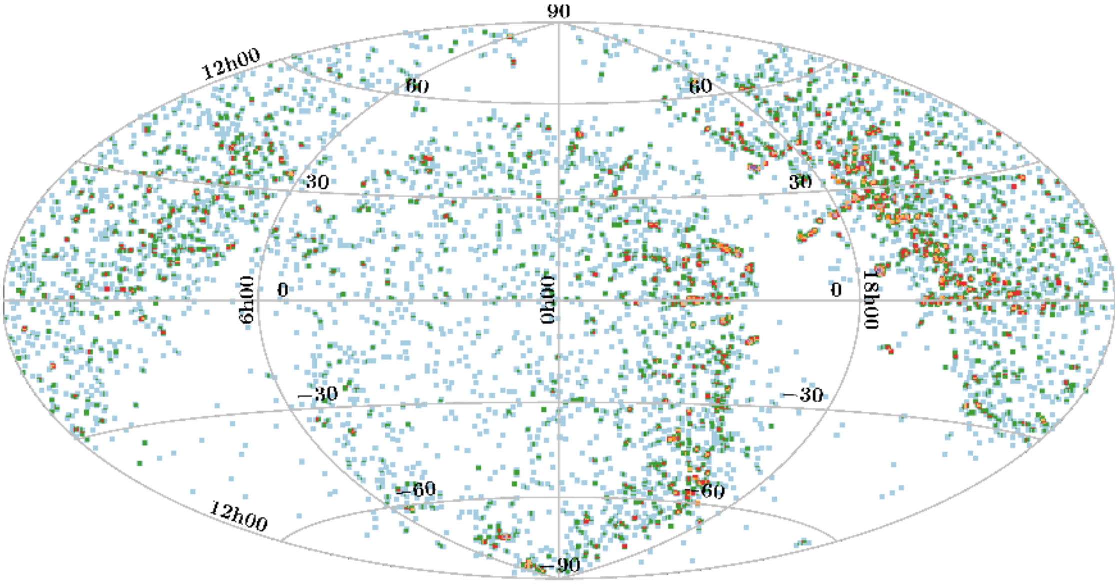

Fig. 2. Sky distribution of the objects in the catalogue in equatorial coordinates. The colour scale represents the densities of the stars starting from green to red, and yellow indicates the most crowded regions.

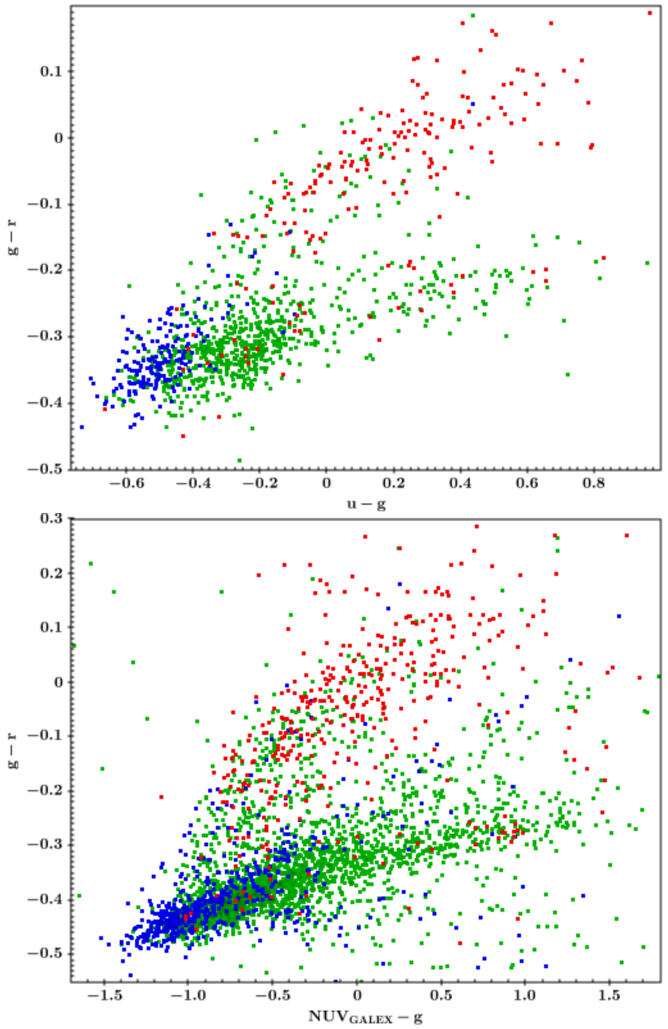

Fig. 3. Two-colour diagrams for spectroscopically classified objects from the hot subdwarf catalogue. The sdB and sdOB stars are indicated in green, sdO stars in blue, and composite binaries in red. *Upper panel*: SkyMapper. *Lower panel*: GALEX/PS1.

Table 1. Colour-classification schemes.

SDSS	
sdO	$-0.55 < u_{\rm SDSS} - g_{\rm SDSS} < -0.35$
	$-0.65 < g_{\rm SDSS} - r_{\rm SDSS} < -0.45$
sdB	$-0.5 < u_{\rm SDSS} - g_{\rm SDSS} < 0.7$
	$g_{\rm SDSS} - r_{\rm SDSS} > 0.208(u_{\rm SDSS} - g_{\rm SDSS}) - 0.516$
	$g_{\rm SDSS} - r_{\rm SDSS} < 0.208(u_{\rm SDSS} - g_{\rm SDSS}) - 0.376$
sd+MS	$-0.5 < u_{\rm SDSS} - g_{\rm SDSS} < 0.7$
	$g_{\rm SDSS} - r_{\rm SDSS} > 0.208(u_{\rm SDSS} - g_{\rm SDSS}) - 0.376$
GALEX/APASS	
sdO/B	$\mathrm{NUV}_{\rm GALEX} - g_{\rm APASS} < 2.0$
	$g_{\rm APASS} - r_{\rm APASS} < -0.15$
sd+MS	$\mathrm{NUV}_{\rm GALEX} - g_{\rm APASS} < 2.0$
	$g_{\rm APASS} - r_{\rm APASS} \geq -0.15$
GALEX/PS1	
sdO/B	$\mathrm{NUV}_{\rm GALEX} - g_{\rm PS1} < 1.7$
	$g_{\rm PS1} - r_{\rm PS1} < -0.2$
sd+MS	$\mathrm{NUV}_{\rm GALEX} - g_{\rm PS1} < 1.7$
	$g_{\rm PS1} - r_{\rm APASS} \geq -0.2$
SkyMapper	
sdO	$-0.8 < u_{\rm SKYM} - g_{\rm SKYM} < -0.4$
	$-0.5 < g_{\rm SKYM} - r_{\rm SKYM} < -0.17$
sdB	$-0.4 < u_{\rm SKYM} - g_{\rm SKYM} < 0.9$
	$-0.5 < g_{\rm SKYM} - r_{\rm SKYM} < -0.17$
sd+MS	$-0.8 < u_{\rm SKYM} - g_{\rm SKYM} < 0.9$
	$-0.17 < g_{\rm SKYM} - r_{\rm SKYM} < 0.3$
BHB	$0.9 < u_{\rm SKYM} - g_{\rm SKYM} < 1.4$
	$0.1 < g_{\rm SKYM} - r_{\rm SKYM} < 0.55$

containing larger samples of sdO/B stars have been taken into account (Heber et al. 1984; Bixler et al. 1991; Saffer et al. 1994, 1997; Maxted et al. 2001; Edelmann et al. 2003; Lisker et al. 2005; Ströer et al. 2007; Hirsch 2009; Østensen et al. 2010b; Nemeth et al. 2012; Geier et al. 2013, 2015a, 2017b; Kupfer et al. 2015; Luo et al. 2016, 2019; Kepler et al. 2016, 2019; Lei et al. 2018, 2019, 2020). Since the main purpose of this catalogue is the identification and classification of hot subdwarf stars, only one set of atmospheric parameters, which is regarded as reliable, is provided for each star even if several different determinations are provided in the literature.

Radial velocities (RVs) are provided for the 2790 stars with spectra in the SDSS and LAMOST data archives. However, for the most helium rich objects, systematic offsets by up to $\sim$100 km s^{-1} are possible owing to cross-correlation with inadequate template spectra (Geier et al. 2015b, 2017a).

3. Summary

The catalogue of known hot subdwarf stars DR2 and the catalogue of objects previously misclassified as hot subdwarfs are both available via the VizieR service. A detailed description of the catalogue columns for both catalogues is provided in Table A.1. The catalogue is by no means complete and heterogeneously selected, which has to be taken into account when using it for statistical analyses. The large samples from LAMOST for example only include single-lined sdO/Bs and the composite sdB+MS binaries are supposed to be published in the future.

DR2 contains 528 newly discovered sdO/B stars and is significantly cleaner than DR1. With the growing number of large-area spectroscopic surveys it is important to keep track of the known objects to allow for a most efficient follow-up of the yet unclassified candidates. The multitude of new designations that comes with each survey does not make this effort easier.

The previously missclassified objects are a mixed bag of interesting and often peculiar stars. The MS-B stars for example are all quite faint and found mostly at high Galactic latitudes. This indicates large distances and a likely runaway origin. Most WDs are likely quite hot, young, and short-lived, and therefore rare.

The *Gaia* catalogue of hot subluminous star candidates will be maintained and updated in parallel (Geier et al. 2019) to provide a comprehensive list of new hot subdwarf candidates. Together with the WD catalogue (Gentile Fusillo et al. 2019) and the catalogue of extremely low-mass WD candidates (Pelisoli & Vos 2019) the whole parameter space of hot subluminous stars is now covered. In addition, we are currently compiling catalogues of variable hot subdwarfs based on the diverse light-curve surveys now available. The first such catalogue including eclipsing HW Vir-type binaries has recently been published by Schaffenroth et al. (2019).

Acknowledgements. I would like to thank the referee Dave Kilkenny for his constructive report. S. G. was supported by the Heisenberg program of the Deutsche Forschungsgemeinschaft (DFG) through grants GE 2506/8-1 and GE 2506/9-1. This research made use of TOPCAT, an interactive graphical viewer and editor for tabular data Taylor (2005). This research made use of the SIMBAD database, operated at CDS, Strasbourg, France; the VizieR catalogue access tool, CDS, Strasbourg, France. Some of the data presented in this paper were obtained from the Mikulski Archive for Space Telescopes (MAST). STScI is operated by the Association of Universities for Research in Astronomy, Inc., under NASA contract NAS5-26555. Support for MAST for non-HST data is provided by the NASA Office of Space Science via grant NNX13AC07G and by other grants and contracts. This research has made use of the services of the ESO Science Archive Facility. This work has made use of data from the European Space Agency (ESA) mission *Gaia* (https://www.cosmos.esa.int/gaia), processed by the *Gaia* Data Processing and Analysis Consortium (DPAC, https://www.cosmos.esa.int/web/gaia/dpac/consortium). Funding for the DPAC has been provided by national institutions, in particular the institutions participating in the *Gaia* Multilateral Agreement. This publication makes use of data products from the Two Micron All Sky Survey, which is a joint project of the University of Massachusetts and the Infrared Processing and Analysis Center/California Institute of Technology, funded by the National Aeronautics and Space Administration and the National Science Foundation. Based on observations made with the NASA Galaxy Evolution Explorer. GALEX is operated for NASA by the California Institute of Technology under NASA contract NAS5-98034. This research has made use of the APASS database, located at the AAVSO web site. Funding for APASS has been provided by the Robert Martin Ayers Sciences Fund. The Guide Star catalogue-II is a joint project of the Space Telescope Science Institute and the Osservatorio Astronomico di Torino. Space Telescope Science Institute is operated by the Association of Universities for Research in Astronomy, for the National Aeronautics and Space Administration under contract NAS5-26555. The participation of the Osservatorio Astronomico di Torino is supported by the Italian Council for Research in Astronomy. Additional support is provided by European Southern Observatory, Space Telescope European Coordinating Facility, the International GEMINI project and the European Space Agency Astrophysics Division. Based on observations obtained as part of the VISTA Hemisphere Survey, ESO Program, 179.A-2010 (PI: McMahon). This publication has made use of data from the VIKING survey from VISTA at the ESO Paranal Observatory, programme ID 179.A-2004. Data processing has been contributed by the VISTA Data Flow System at CASU, Cambridge and WFAU, Edinburgh. Based on data products from observations made with ESO Telescopes at the La Silla Paranal Observatory under program ID 177.A 3011(A,B,C,D,E.F). Based on data products from observations made with ESO Telescopes at the La Silla Paranal Observatory under programme IDs 177.A-3016, 177.A-3017 and 177.A-3018, and on data products produced by Target/OmegaCEN, INAF-OACN, INAF-OAPD and the KiDS production team, on behalf of the KiDS consortium. OmegaCEN and the KiDS production team acknowledge support by NOVA and NWO-M grants. Members of INAF-OAPD and INAF-OACN also acknowledge the support from the Department of Physics & Astronomy of the University of Padova, and of the Department of Physics of Univ. Federico II (Naples). This publication makes use of data products from the Wide-field Infrared Survey Explorer, which is a joint project of the University of California, Los Angeles, and the Jet Propulsion Laboratory/California Institute of Technology, and NEOWISE, which is a project of the Jet Propulsion Laboratory/California Institute of Technology. WISE and NEOWISE are funded by the National Aeronautics and Space Administration. Based on observations collected at the Centro Astronómico Hispano Alemán (CAHA) at Calar Alto, operated jointly by the Max-Planck Institut für Astronomie and the Instituto de Astrofísica de Andalucía (CSIC). Based on observations with the *William Herschel* and *Isaac Newton* Telescopes operated by the Isaac Newton Group at the Observatorio del Roque de los Muchachos of the Instituto de Astrofisica de Canarias on the island of La Palma, Spain. The Pan-STARRS1 Surveys (PS1) and the PS1 public science archive have been made possible through contributions by the Institute for Astronomy, the University of Hawaii, the Pan-STARRS Project Office, the Max-Planck Society and its participating institutes, the Max Planck Institute for Astronomy, Heidelberg and the Max Planck Institute for Extraterrestrial Physics, Garching, The Johns Hopkins University, Durham University, the University of Edinburgh, the Queen's University Belfast, the Harvard-Smithsonian Center for Astrophysics, the Las Cumbres Observatory Global Telescope Network Incorporated, the National Central University of Taiwan, the Space Telescope Science Institute, the National Aeronautics and Space Administration under Grant No. NNX08AR22G issued through the Planetary Science Division of the NASA Science Mission Directorate, the National Science Foundation Grant No. AST-1238877, the University of Maryland, Eotvos Lorand University (ELTE), the Los Alamos National Laboratory, and the Gordon and Betty Moore Foundation. The national facility capability for SkyMapper has been funded through ARC LIEF grant LE130100104 from the Australian Research Council, awarded to the University of Sydney, the Australian National University, Swinburne University of Technology, the University of Queensland, the University of Western Australia, the University of Melbourne, Curtin University of Technology, Monash University and the Australian Astronomical Observatory. SkyMapper is owned and operated by The Australian National University's Research School of Astronomy and Astrophysics. The survey data were processed and provided by the SkyMapper Team at ANU. The SkyMapper node of the All-Sky Virtual Observatory (ASVO) is hosted at the National Computational Infrastructure (NCI). Development and support the SkyMapper node of the ASVO has been funded in part by Astronomy Australia Limited (AAL) and the Australian Government through the Commonwealth's Education Investment Fund (EIF) and National Collaborative Research Infrastructure Strategy (NCRIS), particularly the National eResearch Collaboration Tools and Resources (NeCTAR) and the Australian National Data Service Projects (ANDS). Guoshoujing Telescope (the Large Sky Area Multi-Object Fiber Spectroscopic Telescope LAMOST) is a National Major Scientific Project built by the Chinese Academy of Sciences. Funding for the project has been provided by the National Development and Reform Commission. LAMOST is operated and managed by the National Astronomical Observatories, Chinese Academy of Sciences. Funding for the SDSS and SDSS-II has been provided by the Alfred P. Sloan Foundation, the Participating Institutions, the National Science Foundation, the US Department of Energy, the National Aeronautics and Space Administration, the Japanese Monbukagakusho, the Max Planck Society, and the Higher Education Funding Council for England. The SDSS web site is http://www.sdss.org/. The SDSS is managed by the Astrophysical Research Consortium for the Participating Institutions. The Participating

Institutions are the American Museum of Natural History, Astrophysical Institute Potsdam, University of Basel, University of Cambridge, Case Western Reserve University, University of Chicago, Drexel University, Fermilab, the Institute for Advanced Study, the Japan Participation Group, Johns Hopkins University, the Joint Institute for Nuclear Astrophysics, the Kavli Institute for Particle Astrophysics and Cosmology, the Korean Scientist Group, the Chinese Academy of Sciences (LAMOST), Los Alamos National Laboratory, the Max-Planck-Institute for Astronomy (MPIA), the Max-Planck-Institute for Astrophysics (MPA), New Mexico State University, Ohio State University, University of Pittsburgh, University of Portsmouth, Princeton University, the United States Naval Observatory, and the University of Washington. Funding for SDSS-III has been provided by the Alfred P. Sloan Foundation, the Participating Institutions, the National Science Foundation, and the US Department of Energy Office of Science. The SDSS-III web site is http://www.sdss3.org/. SDSS-III is managed by the Astrophysical Research Consortium for the Participating Institutions of the SDSS-III Collaboration including the University of Arizona, the Brazilian Participation Group, Brookhaven National Laboratory, University of Cambridge, Carnegie Mellon University, University of Florida, the French Participation Group, the German Participation Group, Harvard University, the Instituto de Astrofisica de Canarias, the Michigan State/Notre Dame/JINA Participation Group, Johns Hopkins University, Lawrence Berkeley National Laboratory, Max Planck Institute for Astrophysics, Max Planck Institute for Extraterrestrial Physics, New Mexico State University, New York University, Ohio State University, Pennsylvania State University, University of Portsmouth, Princeton University, the Spanish Participation Group, University of Tokyo, University of Utah, Vanderbilt University, University of Virginia, University of Washington, and Yale University.

References

Alam, S., Albareti, F. D., Allende Prieto, C., et al. 2015, ApJS, 219, 12
Bianchi, L., Herald, J., Efremova, B., et al. 2011, Ap&SS, 335, 161
Bixler, J. V., Bowyer, S., & Laget, M. 1991, A&A, 250, 370
Boudreaux, T. M., Barlow, B. N., Fleming, S. W., et al. 2017, ApJ, 845, 171
Carrillo, A., Hawkins, K., Bowler, B. B., et al. 2020, MNRAS, 491, 4365
Chambers, K. C., Magnier, E. A., Metcalfe, N., et al. 2016, ArXiv e-prints [arXiv:1612.05560]
Chavira, E. 1958, Bol. Obs. Tonantz. Tacub., 2, 15
Chavira, E. 1959, Bol. Obs. Tonantz. Tacub., 2, 3
Cutri, R. M., Skrutskie, M. F., van Dyk, S., et al. 2014, VizieR Online catalogue: II/328
de Jong, J. T. A., Verdoes Klejin, G. A., Boxhoorn, D., et al. 2015, A&A, 582, 62
Downes, R. A. 1986, ApJS, 61, 569
Edelmann, H., Heber, U., Hagen, H.-J., et al. 2003, A&A, 400, 939
Edge, A., Sutherland, W., Kuijken, K., et al. 2013, The Messenger, 154, 32
Gaia Collaboration (Brown, A. G. A., et al.) 2018, A&A, 616, A1
Geier, S., Heber, U., Edelmann, H., et al. 2013, A&A, 557, 122
Geier, S., Kupfer, T., Heber, U., et al. 2015a, A&A, 577, 26
Geier, S., Fürst, F., Ziegerer, E., et al. 2015b, Science, 347, 1126
Geier, S., Østensen, R. H., Nemeth, P., et al. 2017a, A&A, 600, 50
Geier, S., Østensen, R. H., Nemeth, P., et al. 2017b, Open Astron., 26, 164
Geier, S., Raddi, R., Gentile Fusillo, N. P., & Marsh, T. R. 2019, A&A, 621, 38
Gentile Fusillo, N. P., Gänsicke, B. T., & Greiss, S. 2015, MNRAS, 448, 2260
Gentile Fusillo, N. P., Tremblay, P.-E., Gänsicke, B. T., et al. 2019, MNRAS, 482, 4570
Green, R. F., Schmidt, M., & Liebert, J. 1986, ApJS, 61, 305
Hagen, H.-J., Groote, D., Engels, D., & Reimers, D. 1995, A&AS, 111, 195
Han, Z., Podsiadlowski, P., Maxted, P. F. L., Marsh, T. R., & Ivanova, N. 2002, MNRAS, 336, 449
Han, Z., Podsiadlowski, P., Maxted, P. F. L., & Marsh, T. R. 2003, MNRAS, 341, 669
Haro, G., & Luyten, W. J. 1962, Bol. Obs. Tonantz. Tacub., 3, 37
Heber, U. 1986, A&A, 155, 33
Heber, U. 2016, PASP, 128, 082001
Heber, U., Hunger, K., Jonas, G., & Kudritzki, R. P. 1984, A&A, 130, 119
Henden, A. A., Templeton, M., Terrell, D., et al. 2016, VizieR Online Data Catalogue: II/336
Hirsch, H. 2009, PhD Thesis, Friedrich-Alexander University Erlangen-Nürnberg, Germany
Humason, M. L., & Zwicky, F. 1947, ApJ, 105, 85
Iriarte, B., & Chavira, E. 1957, Bol. Obs. Tonantz. Tacub., 2, 3
Kepler, S. O., Pelisoli, I., Koester, D., et al. 2015, MNRAS, 446, 4078
Kepler, S. O., Pelisoli, I., Koester, D., et al. 2016, MNRAS, 455, 3413
Kepler, S. O., Pelisoli, I., Koester, D., et al. 2019, MNRAS, 486, 2169
Kilkenny, D., Heber, U., & Drilling, J. S. 1988, South African Astron. Obs. Circular, 12, 1
Kilkenny, D., O'Donoghue, D., Worters, H. L., et al. 2015, MNRAS, 453, 1879
Kilkenny, D., Worters, H. L., O'Donoghue, D., et al. 2016, MNRAS, 459, 4343
Kupfer, T., Geier, S., Schaffenroth, V., et al. 2015, A&A, 576, 44
Latour, M., Randall, S. K., Calamida, A., Geier, S., & Moehler, S. 2018, A&A, 618, 15
Lawrence, A., Warren, S. J., Almaini, O., et al. 2007, MNRAS, 379, 1599
Lindegren, L., Hernandez, J., Bombrun, A., et al. 2018, A&A, 616, 2
Lisker, T., Heber, U., Napiwotzki, R., Christlieb, N., Han, Z., et al. 2005, A&A, 430, 223
Lei, Z., Zhao, J., Nemeth, P., & Zhao, G. 2018, ApJ, 868, 70
Lei, Z., Zhao, J., Nemeth, P., & Zhao, G. 2019, ApJ, 881, 135
Lei, Z., Zhao, J., Nemeth, P., & Zhao, G. 2020, ApJ, 889, 117
Luo, Y.-P., Nemeth, P., Liu, C., Deng, L.-C., & Han, Z. 2016, ApJ, 818, 202
Luo, Y.-P., Nemeth, P., Deng, L.-C., & Han, Z. 2019, ApJ, 881, 7
Maxted, P. F. L., Heber, U., Marsh, T. R., & North, R. C. 2001, MNRAS, 326, 139
McMahon, R. G., Banerji, M., Gonzalez, E., et al. 2013, The Messenger, 154, 35
Mickaelian, A. M. 2008, AJ, 136, 946
Mickaelian, A. M., Nesci, R., Rossi, C., et al. 2007, A&A, 464, 1177
Nemeth, P., Kawka, A., & Vennes, S. 2012, MNRAS, 427, 2180
O'Donoghue, D., Kilkenny, D., Koen, C., et al. 2013, MNRAS, 431, 240
Oreiro, R., Rodriguez-Lopez, C., Solano, E., et al. 2011, A&A, 530, 2
Østensen, R. H. 2006, Baltic Astron., 15, 85
Østensen, R. H., Silvotti, R., Charpinet, S., et al. 2010a, MNRAS, 409, 1470
Østensen, R. H., Oreiro, R., Solheim, J.-E., et al. 2010b, A&A, 513, 6
Pelisoli, I., & Vos, J. 2019, MNRAS, 488, 2892
Perez-Fernandez, E., Ulla, A., Solano, E., Oreiro, R., & Rodrigo, C. 2016, MNRAS, 457, 3396
Saffer, R. A., Bergeron, P., Koester, D., & Liebert, J. 1994, ApJ, 432, 351
Saffer, R. A., Keenan, F. P., Hambly, N. C., Dufton, P. L., & Liebert, J. 1997, ApJ, 491, 172
Schaffenroth, V., Barlow, B. N., Geier, S., et al. 2019, A&A, 630, 80
Schlafly, E. F., & Finkbeiner, D. P. 2011, ApJ, 737, 103
Shanks, T., Metcalfe, N., Chehade, B., et al. 2015, MNRAS, 451, 4238
Skrutskie, M. F., Cutri, R. M., Stiening, R., et al. 2006, AJ, 131, 1163
Stassun, K. G., Oelkers, R. J., Pepper, J., et al. 2018, AJ, 156, 102
Stobie, R. S., Kilkenny, D., O'Donoghue, D., et al. 1997, MNRAS, 287, 848
Ströer, A., Heber, U., Lisker, T., et al. 2007, A&A, 462, 269
Taylor, M. B. 2005, ASP Conf. Ser., 347, 29
Vennes, S., Kawka, A., & Németh, P. 2011, MNRAS, 410, 2095
Wisotzki, L., Koehler, T., Groote, D., & Reimers, D. 1996, A&AS, 115, 227
Wolf, C., Onken, C. A., Luvaul, L. C., et al. 2018, PASA, 35, 10

Appendix A: Additional table

Table A.1. Catalogue columns.

Column	Format	Description	Unit
NAME	A30	Target name	
GAIA_DESIG	A30	*Gaia* designation	
RA	F10.6	Right ascension (J2000)	deg
Dec	F10.6	Declination (J2000)	deg
GLON	F10.6	Galactic longitude	deg
GLAT	F10.6	Galactic latitude	deg
SPEC_CLASS	A15	Spectroscopic classification	
SPEC_SIMBAD	A15	Spectroscopic classification from SIMBAD	
COLOUR_SDSS	A10	Colour classification SDSS	
COLOUR_APASS	A10	Colour classification GALEX/APASS	
COLOUR_PS1	A10	Colour classification GALEX/PS1	
COLOUR_SKYM	A10	Colour classification SkyMapper	
PLX	F8.4	*Gaia* parallax	mas
e_PLX	F8.4	Error on PLX	mas
M_G	F8.4	Absolute magnitude in *G*-band	mag
G_GAIA	F6.3	*Gaia G*-band magnitude	mag
e_G_GAIA	F6.3	Error on G_GAIA	mag
BP_GAIA	F6.3	*Gaia* BP-band magnitude	mag
e_BP_GAIA	F6.3	Error on BP_GAIA	mag
RP_GAIA	F6.3	*Gaia* RP-band magnitude	mag
e_RP_GAIA	F6.3	Error on RP_GAIA	mag
PMRA_GAIA	F7.3	*Gaia* proper motion $\mu_\alpha \cos\delta$	mas yr^{-1}
e_PMRA_GAIA	F7.3	Error on PMRA_GAIA	mas yr^{-1}
PMDEC_GAIA	F7.3	*Gaia* proper motion μ_δ	mas yr^{-1}
e_PMDEC_GAIA	F7.3	Error on PMDEC_GAIA	mas yr^{-1}
RV_SDSS	F5.1	Radial velocity SDSS	km s^{-1}
e_RV_SDSS	F5.1	Error on RV_SDSS	km s^{-1}
RV_LAMOST	F5.1	Radial velocity LAMOST	km s^{-1}
e_RV_LAMOST	F5.1	Error on RV_LAMOST	km s^{-1}
TEFF	F8.1	Effective temperature	K
e_TEFF	F8.1	Error on T_EFF	K
LOG_G	F4.2	Log surface gravity (gravity in cm s^{-2})	dex
e_LOG_G	F.4.2	Error on LOG_G	dex
LOG_Y	F5.2	Log helium abundance n(He)/n(H)	dex
e_LOG_Y	F5.2	Error on LOG_Y	dex
PARAMS_REF	A20	Reference for atmospheric parameters (Bibcode)	
EB-V	F6.4	Instellar reddening $E(B-V)$	mag
e_EB-V	F6.4	Error on $E(B-V)$	mag
AV	F6.4	Interstellar extinction A_V	mag
FUV_GALEX	F6.3	GALEX FUV-band magnitude	mag
e_FUV_GALEX	F6.3	Error on FUV_GALEX	mag
NUV_GALEX	F6.3	GALEX NUV-band magnitude	mag
e_NUV_GALEX	F6.3	Error on NUV_GALEX	mag
V_APASS	F6.3	APASS *V*-band magnitude	mag
e_V_APASS	F6.3	Error on V_APASS	mag
B_APASS	F6.3	APASS *B*-band magnitude	mag
e_B_APASS	F6.3	Error on V_APASS	mag
g_APASS	F6.3	APASS *g*-band magnitude	mag
e_g_APASS	F6.3	Error on g_APASS	mag
r_APASS	F6.3	APASS *r*-band magnitude	mag
e_r_APASS	F6.3	Error on r_APASS	mag
i_APASS	F6.3	APASS *i*-band magnitude	mag
e_i_APASS	F6.3	Error on i_APASS	mag
u_SDSS	F6.3	SDSS *u*-band magnitude	mag
e_u_SDSS	F6.3	Error on u_SDSS	mag
g_SDSS	F6.3	SDSS *g*-band magnitude	mag
e_g_SDSS	F6.3	Error on g_SDSS	mag
r_SDSS	F6.3	SDSS *r*-band magnitude	mag
e_r_SDSS	F6.3	Error on r_SDSS	mag
i_SDSS	F6.3	SDSS *i*-band magnitude	mag
e_i_SDSS	F6.3	Error on i_SDSS	mag
z_SDSS	F6.3	SDSS *z*-band magnitude	mag
e_z_SDSS	F6.3	Error on z_SDSS	mag

Table A.1. continued.

Column	Format	Description	Unit
u_VST	F6.3	VST surveys (ATLAS, KiDS) *u*-band magnitude	mag
e_u_VST	F6.3	Error on u_VST	mag
g_VST	F6.3	VST surveys (ATLAS, KiDS) *g*-band magnitude	mag
e_g_VST	F6.3	Error on g_VST	mag
r_VST	F6.3	VST surveys (ATLAS, KiDS) *r*-band magnitude	mag
e_r_VST	F6.3	Error on r_VST	mag
i_VST	F6.3	VST surveys (ATLAS, KiDS) *i*-band magnitude	mag
e_i_VST	F6.3	Error on i_VST	mag
z_VST	F6.3	VST surveys (ATLAS, KiDS) *z*-band magnitude	mag
e_z_VST	F6.3	Error on z_VST	mag
u_SKYM	F6.3	SkyMapper *u*-band magnitude	mag
e_u_SKYM	F6.3	Error on u_SKYM	mag
v_SKYM	F6.3	SkyMapper *v*-band magnitude	mag
e_v_SKYM	F6.3	Error on v_SKYM	mag
g_SKYM	F6.3	SkyMapper *g*-band magnitude	mag
e_g_SKYM	F6.3	Error on g_SKYM	mag
r_SKYM	F6.3	SkyMapper *r*-band magnitude	mag
e_r_SKYM	F6.3	Error on r_SKYM	mag
i_SKYM	F6.3	SkyMapper *i*-band magnitude	mag
e_i_SKYM	F6.3	Error on i_SKYM	mag
z_SKYM	F6.3	SkyMapper *z*-band magnitude	mag
e_z_SKYM	F6.3	Error on z_SKYM	mag
g_PS1	F7.4	PS1 *g*-band magnitude	mag
e_g_PS1	F7.4	Error on g_PS1	mag
r_PS1	F7.4	PS1 *r*-band magnitude	mag
e_r_PS1	F7.4	Error on r_PS1	mag
i_PS1	F7.4	PS1 *i*-band magnitude	mag
e_i_PS1	F7.4	Error on i_PS1	mag
z_PS1	F7.4	PS1 *z*-band magnitude	mag
e_z_PS1	F7.4	Error on z_PS1	mag
y_PS1	F7.4	PS1 *y*-band magnitude	mag
e_y_PS1	F7.4	Error on y_PS1	mag
J_2MASS	F6.3	2MASS *J*-band magnitude	mag
e_J_2MASS	F6.3	Error on J_2MASS	mag
H_2MASS	F6.3	2MASS *H*-band magnitude	mag
e_H_2MASS	F6.3	Error on H_2MASS	mag
K_2MASS	F6.3	2MASS *K*-band magnitude	mag
e_K_2MASS	F6.3	Error on K_2MASS	mag
Y_UKIDSS	F6.3	UKIDSS *Y*-band magnitude	mag
e_Y_UKIDSS	F6.3	Error on Y_UKIDSS	mag
J_UKIDSS	F6.3	UKIDSS *J*-band magnitude	mag
e_J_UKIDSS	F6.3	Error on J_UKIDSS	mag
H_UKIDSS	F6.3	UKIDSS *H*-band magnitude	mag
e_H_UKIDSS	F6.3	Error on H_UKIDSS	mag
K_UKIDSS	F6.3	UKIDSS *K*-band magnitude	mag
e_K_UKIDSS	F6.3	Error on K_UKIDSS	mag
Z_VISTA	F6.3	VISTA surveys (VHS, VIKING) Z-band magnitude	mag
e_Z_VISTA	F6.3	Error on Z_VISTA	mag
Y_VISTA	F6.3	VISTA surveys (VHS, VIKING) *Y*-band magnitude	mag
e_Y_VISTA	F6.3	Error on Y_VISTA	mag
J_VISTA	F6.3	VISTA surveys (VHS, VIKING) *J*-band magnitude	mag
e_J_VISTA	F6.3	Error on J_VISTA	mag
H_VISTA	F6.3	VISTA surveys (VHS, VIKING) *H*-band magnitude	mag
e_H_VISTA	F6.3	Error on H_VISTA	mag
Ks_VISTA	F6.3	VISTA surveys (VHS, VIKING) K_s-band magnitude	mag
e_Ks_VISTA	F6.3	Error on Ks_VISTA	mag
W1	F6.3	WISE W1-band magnitude	mag
e_W1	F6.3	Error on W1	mag
W2	F6.3	WISE W2-band magnitude	mag
e_W2	F6.3	Error on W2	mag
W3	F6.3	WISE W3-band magnitude	mag
e_W3	F6.3	Error on W3	mag
W4	F6.3	WISE W4-band magnitude	mag
e_W4	F6.3	Error on W4	mag